

# **Holliday Junctions formed from Human Telomeric DNA**

**Shozeb Haider<sup>†, #, \*</sup>, Pengfei Li<sup>†</sup>, Soraia Khiali<sup>†</sup>, Deeksha Munnur<sup>‡</sup>,  
Arvind Ramanathan<sup>§</sup>, Gary N Parkinson<sup>†, #, \*</sup>**

**SUPPORTING INFORMATION  
FOR  
PUBLICATION**

## Contents:

Branch migration assays using PAGE	Page S3
HJ Stability and Salt Concentration Dependence	Page S3
Figure S1. DNA sequences with predicted and observed HJ topologies.	Page S5
Figure S2. Thermal melt experiments.	Page S6
Figure S3. Schematic representations for modified HJ <sub>3</sub> sequences with mutated sequences positioned within the ACC triplet designed to disrupt dimerization of HJ <sub>3</sub> sequences.	Page S7
Figure S4. Schematic representation of the HJ structures determined in this study.	Page S8
Figure S5. Schematic view of the mobile telomeric Holliday junction (tHJ).	Page S9
Figure S6. Branch migration assays.	Page S10
Figure S7. Native PAGE (17%) mobility studies to investigate conformational dynamics of Holliday	Page S11
Table S1-S2: Data collection and refinement statistics (molecular replacement)	Page S12-13
Table S3: The telomeric Holliday junction (tHJ) oligonucleotide sequences used for branch migration assays.	
Movie S1: Holliday junction formed from 10mer telomeric sequence.	Page S13
Movie S2: Holliday junctions formed from two 42mer HJ <sub>3</sub> telomeric sequences	Page S14
Movie S3: Surface representation of core Holliday junctions.	Page S14

### **Branch migration Assays using PAGE**

For all the branch migration assays conducted the duplex substrates were substantially hybridised through their single-stranded tails before incubation, as evidenced by the appearance 326 bp Holliday junction intermediates at time=0.0 minute (Figure S6). Since the AB strands were only formed when the tHJ has branch migrated, the time course required for strands AB to appear can be used to approximate the tHJ branch migration rate. Across the time course, it was seen that the intensity of the 326 bp Holliday junction intermediates decreased while the corresponding product duplex, AB, increased, indicating that branch migration was taking place.

Given that the electrophoretic mobility of a nucleic acid assembly is a function of its size and shape, we presume the two distinct bands observed near the top of the gel in some of the branch migration assays (Figure S6), corresponded to the higher molecular weight Holliday junction intermediates formed by the component partial duplexes. The upper band most likely represented the Holliday junction intermediate structure after single-stranded tails were hybridised, as the flexure at the junction would retard its electrophoretic mobility (Figure S6). The lower band likely corresponded to the nearly-linear Holliday junction intermediate just before it dissociates into the product duplexes (similar to Figure S6). Strand AB was observed at the earliest time point when branch migration assay was carried out in the absence of divalent cations while it took about 10.0 minutes and 8.0 minutes to appear when assays were carried out in the presence of 50 mM MgCl<sub>2</sub> and 50 mM CaCl<sub>2</sub>, respectively (Figure S6).

### **HJ Stability and Salt Concentration Dependence**

In an effort to characterise the possible folded topologies in solution for our telomeric sequences used in our crystallisation studies we undertook thermal melting and PAGE studies. The addition of divalent cations appears to strongly promote HJ formation for the short HJ<sub>1</sub>AB sequence based on the gel retardation (Figure S7). Changes in the band migrations from the native PAGE (Figure S7) appears to be supported by the thermal melt data (Figure S2). There is a significant increase in the denaturation temperature with the addition of divalent cations, a characteristic of HJs transitioning to a stacked-X form. The addition of > 1 mM Mg<sup>2+</sup> ions were shown to change the conformation of a four-way junction (Cruci3HL) from an Open-X form to the Stacked-X form<sup>1</sup>. We observe a ratio (HJ<sub>1</sub>-AB/dsDNA) without MgCl<sub>2</sub> (67/83) equals 0.74, with MgCl<sub>2</sub>

(40/54) equals 0.81 suggesting a transition from double-stranded duplex to HJ. However, the addition of  $Mg^{2+}$  has no apparent effect on the relative mobility of the HJ<sub>2-3</sub> family of cruciform forming sequences, even when containing modifications to the ACC triplet. Despite the presence of the base modifications in the HJ<sub>3-M</sub> sequences, disrupting the ACC triplet at the HJ step, HJs are still able to form. This in part might be explained by the addition of the stabilizing effect of linking nucleotides between 5' and 3' ends of DNA and that cruciforms have been shown to stably fold as HJs without the requirement of ACC triplets. The mobility observed for our sequences is consistent with a similar cruciform forming sequence (Cruci3HL) that has been shown to transition from open to stacked-X forms<sup>1</sup> in the presence of  $Mg^{2+}$  ions, which has no apparent effect on mobility during PAGE analysis<sup>50</sup>. We do however see a second band appearing (Figure S7) but only for the HJ<sub>2</sub> and HJ<sub>3</sub> sequences in the presence of  $Mg^{2+}$  ions, indicating that a dimer may be forming, consistent with our crystallographic results showing the hybridization of two monomers. The thermal melt experiments also appear consistent with an enhanced stabilization reflected in an increased  $T_m > 73$  °C for HJ<sub>2</sub> and HJ<sub>3</sub> sequences (Figure S2e). When viewed over a range of  $Mg^{2+}$  concentrations the HJ<sub>3</sub> family of cruciform forming sequences (Figure S2(h)) show a strong initial stabilization in 0-2 mM  $Mg^{2+}$  ions that quickly plateaus off HJ<sub>3</sub> > HJ<sub>3-M1</sub> > HJ<sub>3-M2</sub>.

1. Duckett, D. R.; Murchie, A. I.; Diekmann, S.; von Kitzing, E.; Kemper, B.; Lilley, D. M., The structure of the Holliday junction, and its resolution. *Cell* **1988**, *55* (1), 79-89.

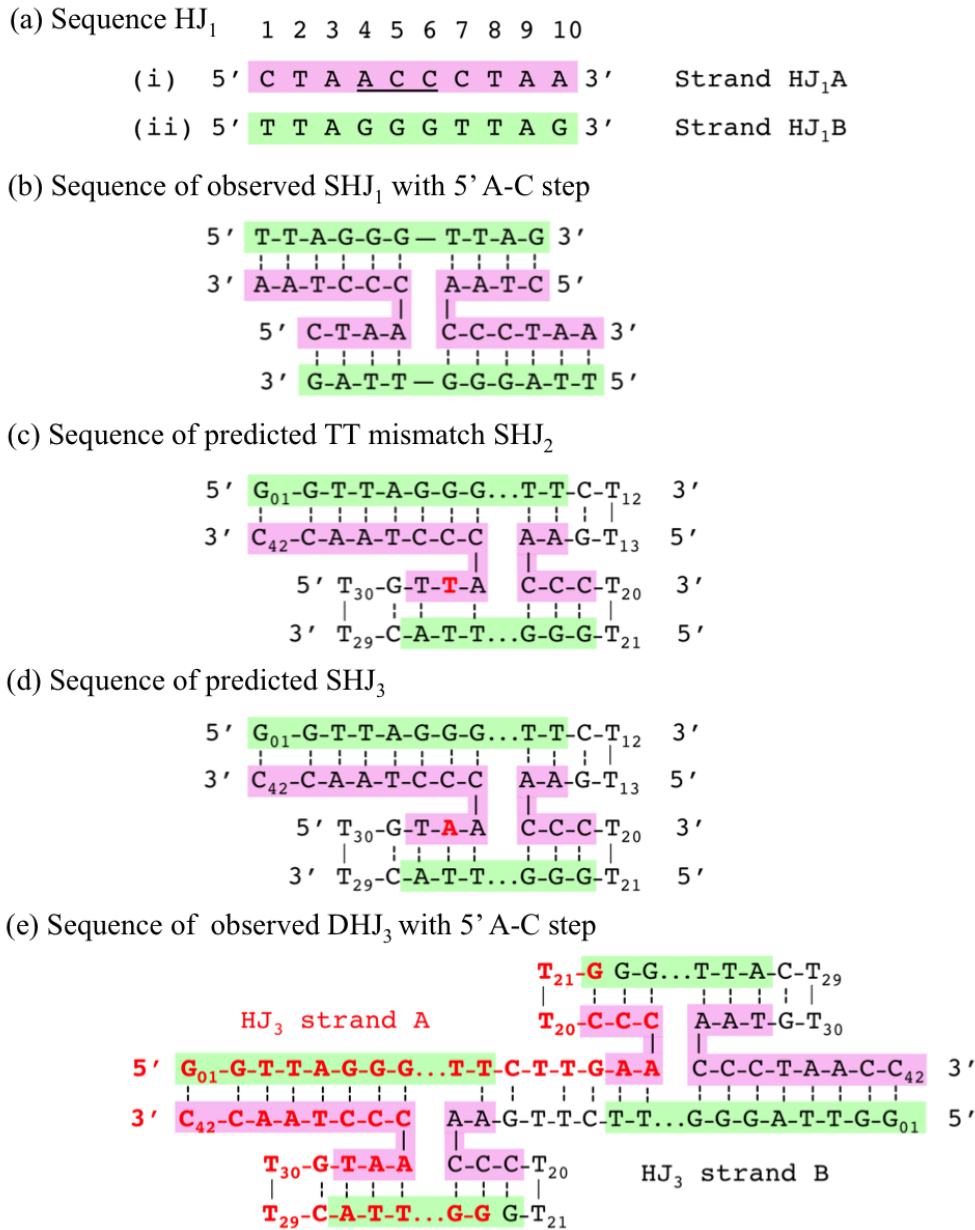


**Figure S1. DNA sequences with predicted and observed HJ topologies.** The C-rich telomeric sequences are highlighted in purple and complimentary G-rich sequences in green. Dashed lines represent hydrogen bonds, solid lines represent backbone covalent linkages. (a) 10mer HJ<sub>1</sub>AB sequences. (b) Schematic representation of SHJ<sub>1</sub> showing the hybridised HJ<sub>1</sub>AB sequences. (c,d) Predicted topologies for 42mer HJ<sub>2</sub> and HJ<sub>3</sub> sequences prior to structural determinations. (e) Schematic representation of DHJ<sub>3</sub> structure as observed in the ASU of space group P2<sub>1</sub>. Two HJ<sub>3</sub> strands (red and black font) hybridise to generate two Holliday junctions in close proximity.

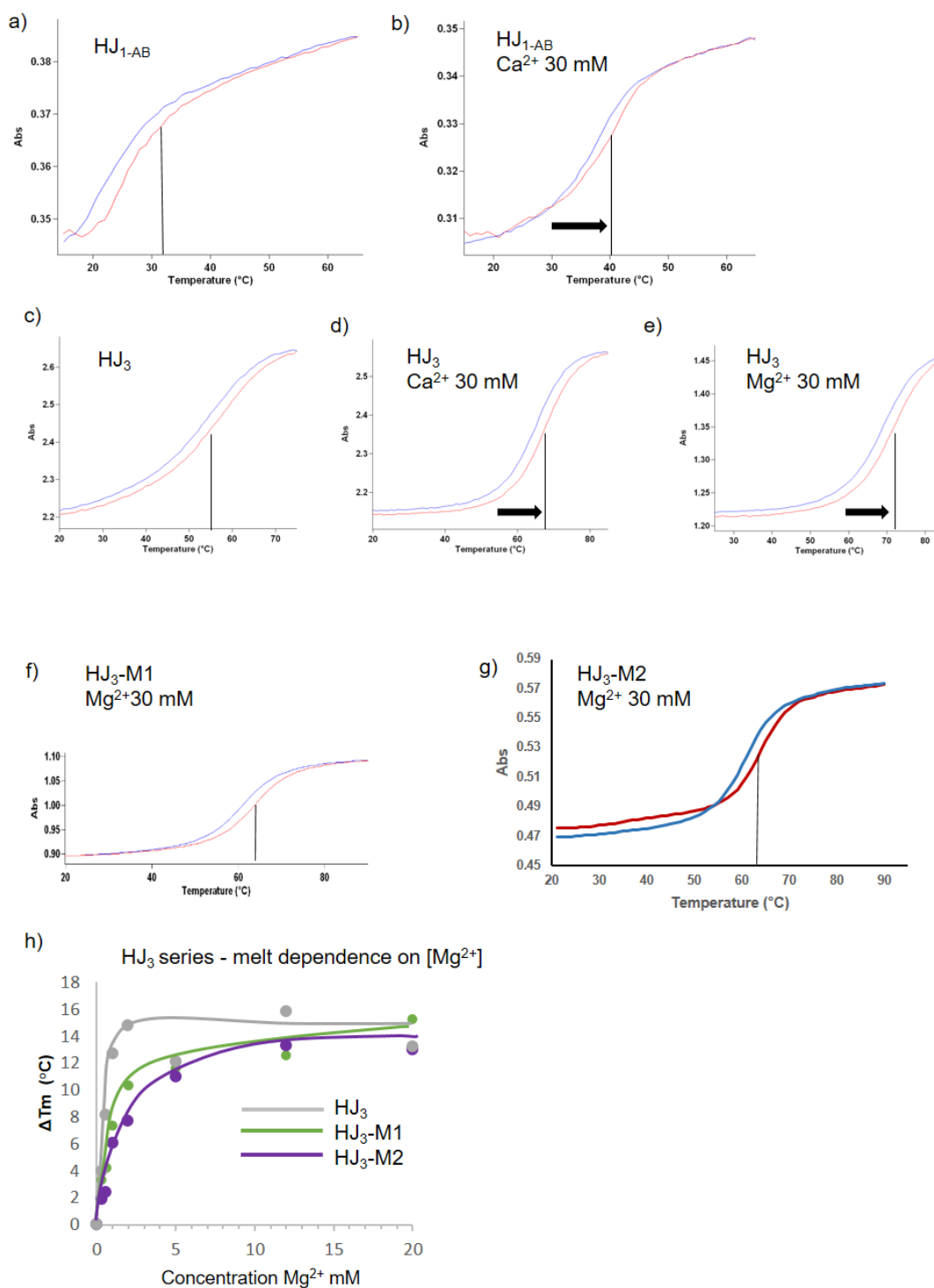


**Figure S2. Thermal melt experiments.** Absorbance measured at 260 nm, red melt and blue annealing. (a) HJ<sub>1</sub>AB, without Mg<sup>2+</sup> (b) HJ<sub>1</sub>AB with the addition of Ca<sup>2+</sup> 30 mM. (c) HJ<sub>3</sub> without Mg<sup>2+</sup>. (d) HJ<sub>3</sub> with the addition of Ca<sup>2+</sup> 30 mM and (e) HJ<sub>3</sub> with the addition of Mg<sup>2+</sup> 30 mM. (f) HJ<sub>3</sub>-M1 with the addition of Mg<sup>2+</sup> 30 mM. (g) HJ<sub>3</sub>-M2 with the addition of Mg<sup>2+</sup> 30 mM. (h) HJ<sub>3</sub>, HJ<sub>3</sub>-M1 and HJ<sub>3</sub>-M2 sequences and their change in melt temperature vs Mg<sup>2+</sup> ion concentration.

(a) Sequence HJ<sub>3</sub>-M1

```

1 2 3 4 5 6 7 8 9 10 11 12 13 14 15 16 17 18 19 20 1 2 3 4 5 6 7 8 9 30 1 2 3 4 5 6 7 8 9 40 1 2
5'  G G T T A G G G A T C T T G A T G C C C T T G G C T T A C T T G T T A C C C T A A C C 3'

```

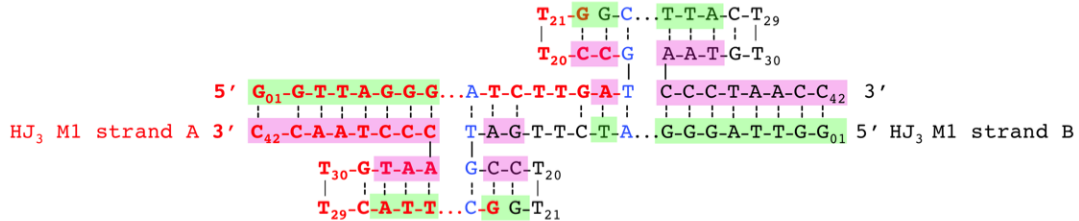
(b) Sequence HJ<sub>3</sub>-M2

```

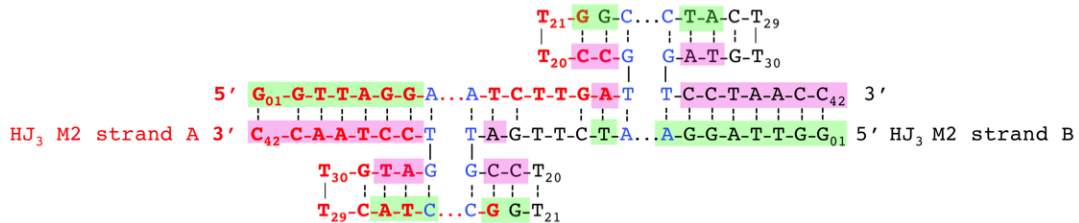
1 2 3 4 5 6 7 8 9 10 11 12 13 14 15 16 17 18 19 20 1 2 3 4 5 6 7 8 9 30 1 2 3 4 5 6 7 8 9 40 1 2
5'  G G T T A G G A A T C T T G A T G C C C T T G G C C T A C T T G T A G T C C T A A C C 3'

```

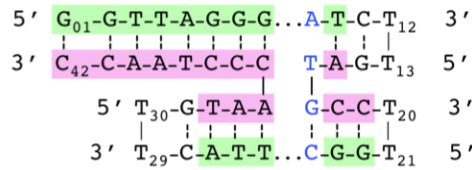
(c) Sequence HJ<sub>3</sub>-M1 folded as HJ



(d) Sequence HJ<sub>3</sub>-M2 folded as HJ



(e) Sequence HJ<sub>3</sub>-M1 folded as HJ

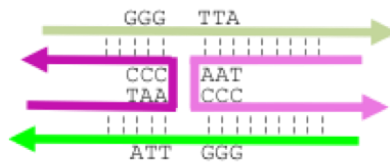


(f) Sequence HJ<sub>3</sub>-M2 folded as HJ



**Figure S3. Schematic representations for modified HJ<sub>3</sub> sequences with mutated sequences positioned within the ACC triplet designed to disrupt dimerization of HJ<sub>3</sub> sequences.** (a) 42mer HJ<sub>3</sub>-M1 sequence. (b) 42mer HJ<sub>3</sub>-M1 sequence. (c) Insertion of a TG step at position 16-17 (blue) (ACC to TGC). (d) Insertion of TG steps at positions 16-17 and 34-35 (blue). (e) Predicted topology for sequence HJ<sub>3</sub>-M1 based on 10mer HJ<sub>1</sub>AB. (f) Topology for sequence HJ<sub>3</sub>-M2 based on 10mer HJ<sub>1</sub>AB.

(a) Schematic representation of the SHJ<sub>1</sub> topology



(b) Schematic representation of DHJ<sub>3</sub> topology

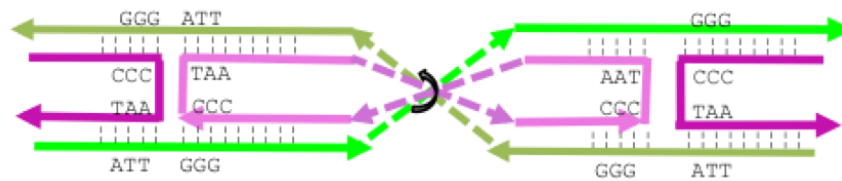


**Figure S4. Schematic representation of the HJ structures determined in this study.** (a) Single HJ (b) Two HJs in close proximity. The solid arrowhead represents the 3' end. The coloured dashed lines represent the links between the strands. The black arrow indicates the rotation of one HJ with respect to the other. The black dashed lines are representative of the hydrogen bond.

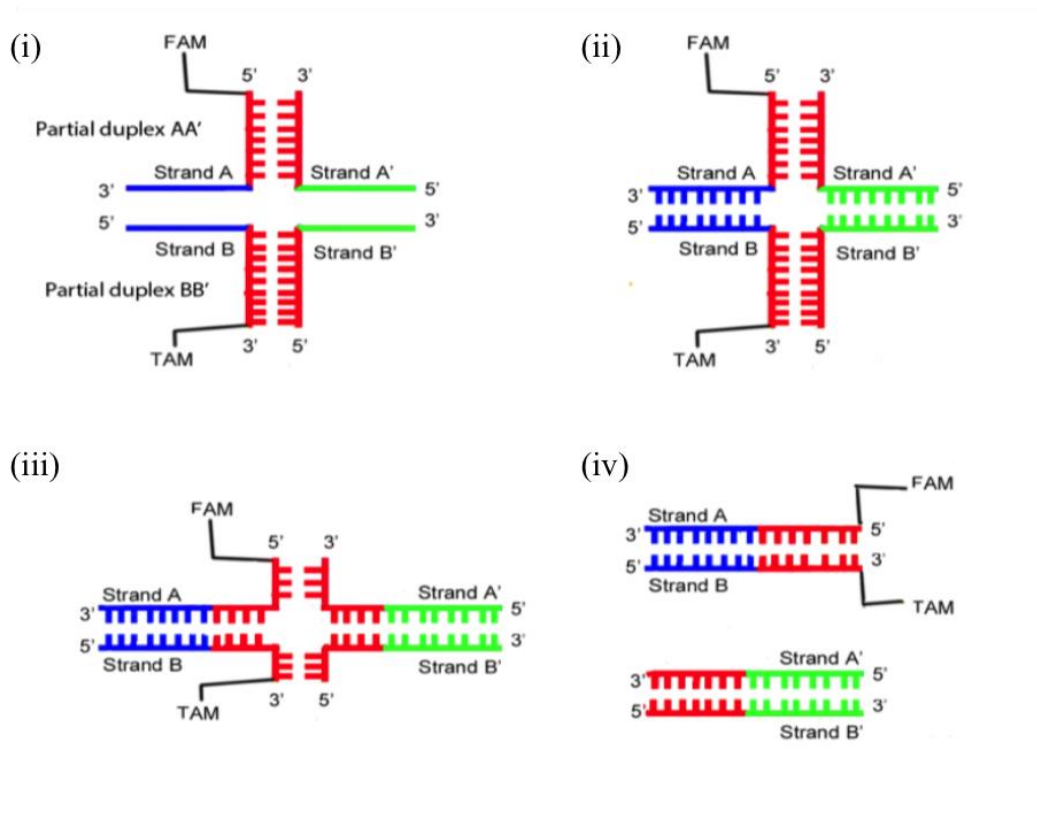


**Figure S5. Schematic view of the mobile telomeric Holliday junction (tHJ).** Different colours are used to indicate sequence complementarity; the parts of the strands with the same colour have complementary sequences. There are 3 continuous telomeric hexanucleotide repeat in strand A at the homologous duplex region. (i) The complementary single-stranded tails are annealed and a mobile telomeric Holliday junction intermediate (326 bp) is formed. (ii) Once spontaneous branch migration is initiated, (iii) there is an exchange of hydrogen bond between the bases in the homologous duplex regions. (iv) Spontaneous branch migration is terminated when strand exchange reached the distal end of the duplex region and the telomeric Holliday junction intermediate is irreversibly dissociated into two linear duplex products, FRET-AB (160 bp, attached with FAM and TAM) and FRET-A'B' (166 bp).

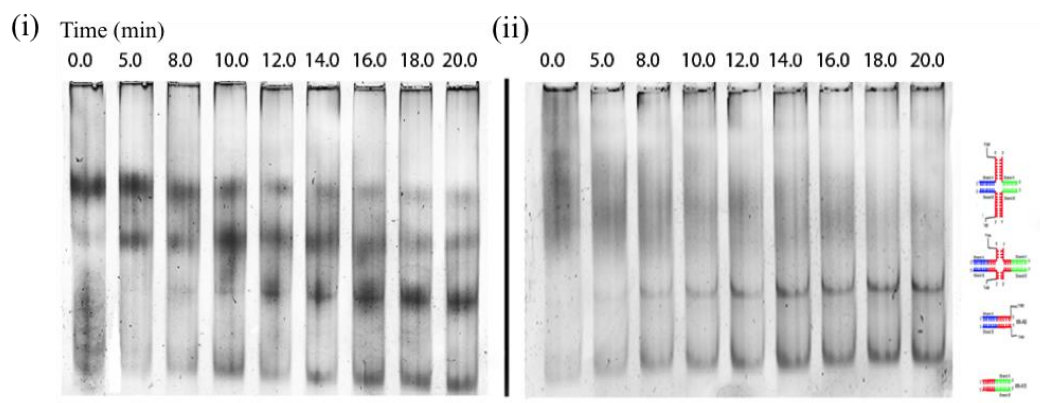


**Figure S6. Branch migration assays.** Carried out in the presence of (i) 50 mM  $Mg^{2+}$  and (ii) 50 mM  $Ca^{2+}$ . The length of incubation at 37.4 °C for the samples is indicated at the top of the lanes.  $Mg^{2+}$  ions show a greater retarding effect on branch migration than  $Ca^{2+}$ . The predicted structures have been illustrated adjacent to their corresponding band positions (Figure S5).

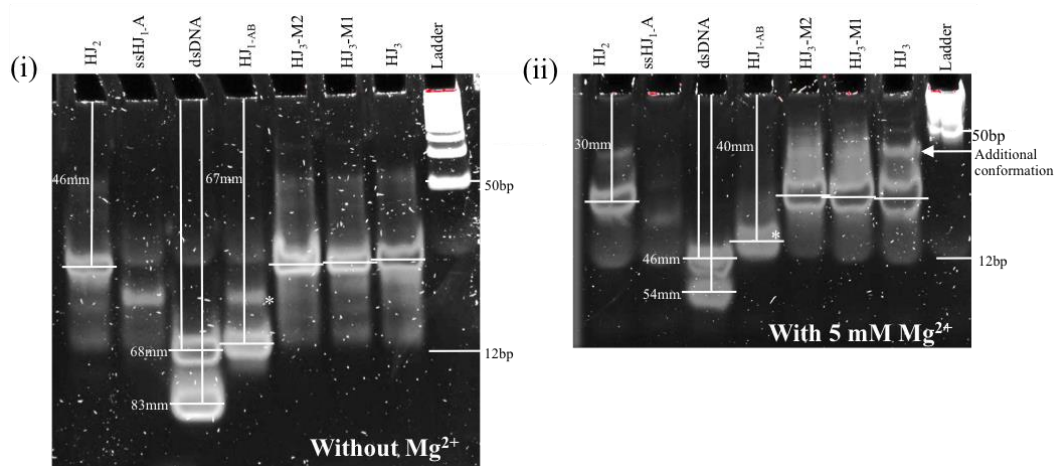


**Figure S7. Native PAGE (17%) mobility studies to investigate conformational dynamics of Holliday junctions** containing telomeric sequences, (i) without  $MgCl_2$  or, (ii) with 5 mM  $MgCl_2$ . The addition of  $Mg^{2+}$  has no apparent effect on the mobility of the  $HJ_3$  family of sequences when the branches are linked together, consistent with similar cruciform forming sequences<sup>50</sup>. While the mobility of  $HJ_{1AB}$  is significantly impacted by the addition of  $Mg^{2+}$ , Ratio ( $HJ_{1AB}/dsDNA$ ), without  $MgCl_2$  ( $67/83$ ) = 0.74, with  $MgCl_2$  ( $40/54$ ) = 0.81 suggesting a transition from double-stranded duplex to  $HJ^*$ .

## Supplementary Tables

**Table S1: Data collection and refinement statistics (molecular replacement)**

	SHJ <sub>1</sub> -1	SHJ <sub>1</sub> -2	SHJ <sub>1</sub> -3
<b>Data collection</b>			
Space group	P <sub>1</sub>	C 1 2 1	P <sub>1</sub>
Cell dimensions			
<i>a</i> , <i>b</i> , <i>c</i> (Å)	23.733, 33.161, 83.467	62.01, 23.54, 84.11	23.334, 33.183, 41.303
$\alpha$ , $\beta$ , $\gamma$ (°)	99.87, 90.07, 110.94	90.00, 99.06, 90.00	99.27, 90.00, 110.59
Resolution (Å)	22.5- 2.80 (2.91-2.80)	30.6-2.982(3.06-2,98)	15.74-2.80(2.95-2.8)
<i>R</i> <sub>sym</sub> or <i>R</i> <sub>merge</sub>	5.6 (37.5)	6.6(74.1)	11.4(33)
<i>I</i> / $\sigma$ <i>I</i>	14.5 (1.6)	8.5(1.3)	5.6 (1.5)
Completeness (%)	97.8 (92.2)	90.0(90.8)	93 (96.5)
Redundancy	3.5 (2.4)	3.0(3.3)	1.8 (1.8)
<b>Refinement</b>			
Resolution (Å)	22.5-2.85	25-3.5	15.74-2.95
No. reflections	5115	1430	2083
<i>R</i> <sub>work</sub> / <i>R</i> <sub>free</sub>	22.7.5/27.3	29.5/35.5	24.4/28.6
No. atoms			
DNA	1616	808	808
Ligand/ion	0	0	0
Water	0	0	0
<i>B</i> -factors			
DNA	43	87	72
Ligand/ion			
R.m.s. deviations			
Bond lengths (Å)	0.008	0.005	0.010
Bond angles (°)	1.55	1.24	1.45

\*Number of xtals for each structure should be noted in footnote. \*Values in parentheses are for highest-resolution shell.

**Table S2:** Data collection and refinement statistics (**molecular replacement**)

	DHJ <sub>2</sub>	DHJ <sub>3</sub>
<b>Data collection</b>		
Space group	P 1 2 <sub>1</sub> 1	P 1 2 <sub>1</sub> 1
Cell dimensions		
<i>a</i> , <i>b</i> , <i>c</i> (Å)	48.3013, 45.9128, 62.4669	49.937, 45.374, 63.828
$\alpha$ , $\beta$ , $\gamma$ (°)	90.00, 99.2863, 90.00	90.00, 101.01, 90.00
Resolution (Å)	24-3.00 (3.11-3.00) *	49-2.69 (2.74-2.69)
<i>R</i> <sub>sym</sub> or <i>R</i> <sub>merge</sub>	10.5 (60)	5.4 (64)
<i>I</i> / $\sigma$ <i>I</i>	17.4 (0.8)	10.9 (1.6)
Completeness (%)	99.7 99.4	99.9 (97.6)
Redundancy	6.1 (5.5)	3.6 (3.7)
<b>Refinement</b>		
Resolution (Å)	30-3.0	49-3.0
No. reflections	5294	5446
<i>R</i> <sub>work</sub> / <i>R</i> <sub>free</sub>	24.6/31.8	23.6/27.9
No. atoms		
DNA	1710	1712
Ligand/ion	2	2
<i>B</i> -factors		
Protein	79	68
Ligand/ion		49
R.m.s deviations		
Bond lengths (Å)	0.008	0.008
Bond angles (°)	1.48	1.56

\*Values in parentheses are for highest-resolution shell.

**Table S3:** The telomeric Holliday junction (tHJ) oligonucleotide sequences used for branch migration assays. The telomeric 5' – TTAGGG – 3' are emphasised in Grey

Name	Number of residues	Oligonucleotide sequences
tHJ	326	Strand A: 5' – (FAM) CGA TCA GGC AGT GAC TCG TCT TAT TAG GGT TAG GGT TAG GGT GAC GGA CGA CAC CTA GCC ACG ACT TCC TCG ACT TCC TC- 3' Strand A': 5' – GCG CGC TCA TTC TCC TCA TTC TCA GTG GCT AGG TGT CGT CCG TCA CCC TAA CCC TAA CCC TAA TAA GAC GAG TCA CTG CCT GAT CG – 3' Strand B: 5' – GAG GAA GTC GAG GAA GTC GTG GCT AGG TGT CGT CCG TCA CCC TAA CCC TAA CCC TAA TAA GAC GAG TCA CTG CCT GAT CG (TAM) – 3' Strand B': 5' – CGA TCA GGC AGT GAC TCG TCT TAT TAG GGT TAG GGT TAG GGT GAC GGA CGA CAC CTA GCC ACT GAG AAT GAG GAG AAT GA – 3'

## Supplementary Movies:

### Movie S1

Movie-1-SHJ<sub>1</sub>-1.mp4 (32 secs)

**Holliday junction formed from 10mer telomeric sequence.** The telomeric G-rich (5'-TTAGGGTTAG-3') and the C-rich strands (5'-CTAACCTAA-3') have been highlighted. The ACC nucleotides in the crossover motif have been labelled.

### Movie S2

Movie-2-DHJ<sub>3</sub>.mp4 (45 secs)

**Holliday junctions formed from two 42mer HJ<sub>3</sub> telomeric sequences.** Nucleotides that were not a part of the telomeric sequence, in HJ<sub>3</sub>, have been omitted for clarity purposes (uncoloured nucleotides in Fig. S1c). The coordinates are extracted from the crystallographic ASU where two Holliday Junctions form in close proximity and resemble the topology of a hemicatenated double Holliday Junction. It is important to note that the two Holliday junctions are independent of any crystallographic symmetry operators. The telomeric G-rich and the C-rich strands have been coloured, and the ACC nucleotides in the crossover motif have been labelled. The spheres illustrate the continuity of the G-rich strands between the HJ helices (olive green and green) and the resulting complex interrelationship when two adjacent Holliday junctions associate to form a hemicatenated double Holliday junction. The two C-rich strands (pink) would also be linked in a hemicatenated double Holliday junction structure.

### Movie S3

Movie-3-DHJ<sub>3</sub>.mp4 (44 secs)

**Surface representation** of the core x-ray determined Holliday Junction structure is shown and then extended on the 5' and 3' ends (by B-DNA) to illustrate the overall geometry of two Holliday junctions in close proximity. The overall topology of the model resembles that of a hemicatenated double Holliday junction.